https://doi.org/10.15407/ujpe71.1.55

T.A. PROKOFIEV, A.V. IVANCHENKO

Oles Honchar National University of Dnipro
(72, Nauky Ave., Dnipro 49010, Ukraine; e-mail: tichonprok@yahoo.de)

RESOLUTION OF LUMINESCENCE SPECTRA INTO SEPARATE COMPONENTS: THE CURVE SHAPE AND THE COORDINATE CHOICE

Based on the configuration coordinate model, the possibility of using individual bands of normal distribution in the photon-energy coordinates to approximate luminescence spectra has been analyzed. The practical application of this approach to ZnS single crystals doped with Mn^{2+} ions made it possible to obtain photoluminescence spectra of individual bands at various plastic deformations. Taking into account the dependence of the area under the individual band curve on the number of luminescence centers allowed us to trace, in a certain way, the change in the relative quantitative characteristics of radiating manganese centers with various local environments during the plastic deformation process. The obtained results correlate with the results of electron paramagnetic resonance studies, supplement the information on the methods for resolving experimental luminescence spectra into individual components, and do not contradict generally accepted ideas about the photoluminescence mechanisms in single-crystalline materials of the A_2B_6-type.

K e y w o r d s: luminescence spectra, luminescence bands, configurational coordinate model, resolution of luminescence spectra into separate components, resolution error of experimental luminescence spectra, plastic deformation.

1. Introduction

The luminescence spectra of most single-crystal materials, for example, compounds of the A_2B_6-type, with dimensions significantly exceeding the crystal lattice constant, are usually broad bands caused by the emission from a large number of luminescence centers, which are located at various sites of the crystal lattice and have different local environments. In fact, those bands can be considered as the sum of several luminescence bands, and each of the latter is associated with the emission by a group of centers with a certain type of local symmetry. This approach allows us, to some extent, to solve the problem of classifying luminescence centers and predict changes in the luminescent properties of the examined materials under various changes in experimental conditions. In this case, individual luminescence bands can be resolved in different ways from the total experimental spectrum.

Two directions can be conditionally distinguished. In one of them, individual bands are attempted to be resolved directly in the course of experiments [1]. The procedure is associated with a rather laborious reconfiguration of the measurement equipment and, in any case, requires further experimental data processing.

Another direction involves the resolution of individual bands by analyzing the obtained experimental spectra. This direction includes the well-known Alentsev–Fock method [2]. The latter makes it possible to determine the maxima of individual bands

C i t a t i o n: Prokofiev T.A., Ivanchenko A.V. Resolution of luminescence spectra into separate components: the curve shape and the coordinate choice. *Ukr. J. Phys.* **71**, No. 1, 55 (2026). https://doi.org/10.15407/ujpe71.1.55.

and, in some cases, obtain some information about the shape of an individual band contour. However, despite all its advantages, it is rather difficult for practical applications. In particular, it is necessary to search for horizontal sections in the plots for the ratio between the studied experimental spectra, which are used to determine the resolution coefficients necessary for constructing individual luminescence bands. These horizontal sections are detected only if there are quite noticeable differences in the contour shapes of the studied experimental spectra, but the latter are often impossible to obtain without considerable changes in experimental conditions. Furthermore, the accuracy of determining the contour shape of an individual band and the accuracy of resolution as a whole largely depend on the experimental spectrum registration accuracy. This task is quite laborious by itself, being hard to automate, especially if the number of individual bands is large. This fact complicates the construction of adequate luminescence models illustrating the behavior of luminescent materials at minor changes in the contour shape of experimental spectra as a result of changes in excitation conditions.

In our opinion, the most promising approach in the latter direction is the application of approximation resolution methods [3–10]. Due to a high automation level, those methods allow processing a substantial body of experimental data within a fairly short time interval. This makes it possible to obtain statistically significant results without substantial resource costs and a reconfiguration of measuring equipment, and significantly simplifies the entire research process. However, there are some difficulties here. In particular, to date, there is no unambiguous answer to the question concerning the contour shape of an individual band. Therefore, the issue of choosing approximation functions $f_i(x)$ and, as a result, the procedure of finding their optimal parameters is very problematic, which in turn makes this procedure substantially more difficult and generally complicates the construction of adequate models for individual luminescence bands of researched materials. The purpose of this work is a detailed study of this issue.

2. Theoretical Part

In the general case, when using approximation resolution methods, experimental luminescence spectra are represented as the sum of some functions that describe individual bands, taking into account the error:

$$I(x) = f_1(x) + f_2(x) + f_3(x) + ... + f_n(x) + \Delta\varphi(x). \quad (1)$$

Here $f_i(x)$, $\overline{i = 1, n}$, are functions describing individual bands in the total experimental luminescence spectrum; $\Delta\varphi(x)$ is the resolution error, which is a function describing the deviation of the envelope of the sum of individual bands from the total experimental luminescence spectrum. The parameters of the functions $f_i(x)$ in Eq. (1) are usually selected using one of the optimization methods, for example, using the least squares method [11–13]. Its essence is to minimize a special objective function, the arguments of which are the parameters of the functions $f_i(x)$,

$$\Phi(r_{ik}) = \sum_{j=1}^{m} [I_j(x_j) - \sum_{i=1}^{n} [f_i(x_j)]]^2 = \min, \quad (2)$$

where the subscript $i = \overline{1, n}$ enumerates individual bands, the subscript k enumerates parameters of the functions $f_i(x)$, $I_j(x_j)$ is the intensity of the experimental spectrum at the measurement point x_j, and the subscript $j = \overline{1, m}$ enumerates experimental points in the total experimental luminescence spectrum.

The number of functions $f_i(x)$ in Eq. (1) is determined by the number of types of emitting centers and the known types of their local symmetry, which are usually found by comparing the results of several research methods. For example, when finding these parameters for luminescent single crystals ZnS : Mn, data from chemical analysis, luminescence under excitation of various types, various impurity concentrations and temperatures, electron paramagnetic resonance, X-ray structural analysis, plastic deformation, and annealing of specimens in various environments were used [14–20].

The area under the curve of the function $f_i(x)$ is proportional to the number of emitting centers that radiate into the corresponding individual luminescence band. The maxima of individual bands often appear as peaks in the experimental luminescence spectrum, or they are found based on the alone results of other studies, for example, using the Alentsev–Fock method [2].

In the absence of information about the contour shape of an individual band, the problem of finding the parameters of the functions $f_i(x)$ in Eq. (1) has practically no unique solution, since the number of

variants of the examined functions and, moreover, the number of parameters in those functions tends to infinity. Therefore, additional criteria are needed that restrict the number of variants to analyze. One such criteria can be obtained based on the consequences of the central limit theorems, a class of theorems of probability theory. According to this criterion, the sum of a large number of independent and random variables has a distribution close to normal (Gaussian). Taking into account the large number of luminescence centers, the use of this distribution to describe the contour shape of the functions $f_i(x)$, which is close to the contour shape of an individual band, is quite justified. Since this is the normal distribution just over the transition energies from the excited state to the ground state that has a physical meaning, it is pertinent to apply the photon energy scale as the x-coordinate. In this case, the area under the curve of an individual band, which is proportional to the number of emitting centers, will have the physical meaning of the total radiation energy in an individual band, i.e., the number of photons multiplied by their energy.

However, there is an important circumstance that cannot be ignored. The system of luminescent emitting centers does not exist. It is some part of a metasystem, which is called the crystal lattice of a luminescent material. Such a metasystem affects the distribution of emitting quanta. As a result, the contour shape of an individual band will be somewhat different from the Gaussian one. This was well demonstrated by the analysis in the framework of the configurational coordinate model [2], where the ground and excited energy levels are described in the form of configurational parabolas. Moreover, according to Ref. [2], when considering such a model, it is easy to conclude that the luminescence spectrum can have a Gaussian shape in the energy coordinates only if the section of the potential curve for the ground state located under the region of the excited state minimum can be replaced by a straight segment. (We can also note that the parabolic shape of the excited state curve affects this.) In all other cases, the luminescence spectrum does not have an exact Gaussian shape. That is, taking into account the above and due to the action of phonon or other effects, we may say that the Gaussian shape of an individual band in the photon-energy coordinates is a specific case rather than a rule. Furthermore, if there is no

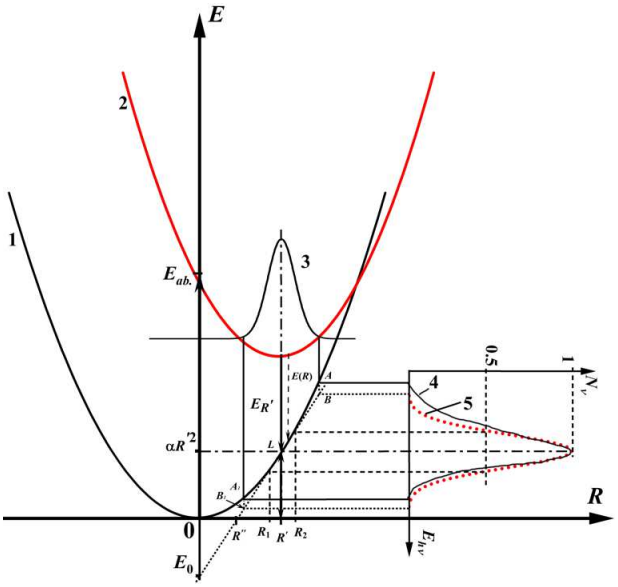

Fig. 1. Configuration coordinate model and the construction of the contour shape for an individual band in the emission spectrum: E is the system energy, R is the configuration coordinate, curve *1* is the potential energy of the luminescence center in the ground state, curve *2* is the potential energy of the luminescence center in the excited state, curve *3* is the probability distribution for the configuration coordinate in the excited state, curve *4* is the theoretical form of the luminescence spectrum of an individual band in the coordinates of photon energies $E_{h\nu}$ on the abscissa axis and the relative number of luminescence centers N_ν on the ordinate axis, and curve *5* is the shape of a resolved individual band in the coordinates of photon energies $E_{h\nu}$ along the abscissa axis

additional information about the shape of individual bands, then it is not known in which coordinates the complex band should be analyzed when resolving it into Gaussian components [2].

Despite all that, in our opinion, a similar model of the ground and excited energy levels of the luminescence centers in the configuration coordinates can be used as another criterion that restricts the number of variants when determining the parameters of the functions $f_i(x)$ in Eq. (1).

In order to assess how much the shape of an individual luminescence band differs from the Gaussian one if the influence of the crystal lattice is taken into account, a model of configuration coordinates with the center located at the minimum of the configuration parabola (the zero point in Fig. 1), which characterizes the ground state, was constructed and

analyzed. In this case, the axis of parabola 1 coincides with the coordinate axis in the energy scale (Fig. 1). As the coordinates of individual bands, we consider the relative number of luminescence centers N_{nu} along the ordinate axis, and the photon energy $E_{h\nu}$ along the abscissa axis (the inset in Fig. 1).

When constructing the model, we assumed that electron transitions do not have phonon repetitions, and the temperature is low enough so that all emitting centers are in the ground vibrational state, and the Franck–Condon principle, according to which atoms have no time to shift during an electron transition, is obeyed. Therefore, in our model, electron transitions are exhibited as vertical straight lines. We also assumed that the possibility of a radiative electron transition depends on the configuration coordinate. In this case, it is convenient to use a quadratic function, which is often used in mathematical analysis, to describe the configuration parabolas,

$$y = ax^2 + bx + c, \tag{3}$$

where the coefficients a, b, and c affect the width (the flatness degree), the shift with respect to the x-axis, and the intersection of the branches with the y-axis, respectively. Then the parabolas describing the ground and excited states (curves *1* and *2*, respectively, in Fig. 1) are given by the expressions

$$\begin{aligned} &E_1(R) = \alpha R^2; \\ &E_2(R) = \beta(R - R')^2 + \alpha R'^2 + E_{R'}. \end{aligned} \tag{4}$$

So, the coefficients b and c (3) are equal to 0 for $E_1(R)$, and $b = -2\beta R'$ and $c = E_{(R')} + \alpha R'^2 + \beta R'^2$ for $E_2(R)$. The transition energy from the excited state to the ground state is defined as the difference

$$\begin{aligned} &E_{h\nu}(R) = E_2(R) - E_1(R) = \\ &= \beta(R - R')^2 + \alpha(R'^2 - R^2) + E_{R'}. \end{aligned} \tag{5}$$

The domain of the function $E_{h\nu}(R)$ lies between the abscissas of the intersection points A and $A1$ of the probability distribution curve of transitions from the excited state to the ground state (curves *2* and *3* in Fig. 1).

If the transition probability distribution for the configuration coordinate (curve *3* in Fig. 1) has the Gaussian shape [4]

$$P(x) = \frac{1}{\sqrt{2}\pi\omega \ \exp\left[\frac{(x-x')^2}{2\omega^2}\right]}, \tag{6}$$

where ω is a parameter characterizing the scattering, then the approximating function $f(x)$ in the selected coordinates of the individual bands (curve *4* in Fig. 1) takes the form

$$N(E_{h\nu}) = A \exp \frac{-[E_{h\nu}(R) - E_{R'}]^2}{2{\omega_R}^2}. \tag{7}$$

In expression (7), the quantity ω_R equals

$$\begin{aligned} &\omega_R = E_{h\nu}(R_1) - E_{h\nu}(R_2) = \\ &= E_2(R_1) - E_1(R_1) - (E_2(R_2) - E_1(R_2)) = \\ &= \alpha(R_2^2 - R_1^2). \end{aligned}$$

Taking into account Eq. (5) and expressing the transition energy in terms of the configuration coordinate R, we obtain the following expression for the shape of the individual luminescence band:

$$\begin{aligned} N(R) = &\frac{p}{\sqrt{2}\pi\alpha(R_2 - R_1)} \times \\ \times \exp &\frac{-[\beta(R - R')^2 + \alpha(R'^2 - R^2)]^2}{2[\alpha(R_2^2 - R_1^2]^2}. \end{aligned} \tag{8}$$

As one can see, the obtained expression is an asymmetric function of R', so curve *4* in Fig. 1 corresponding to expression (8) is somewhat different from the Gaussian form. The practical application of expression (8) in the model described by formulas (1) and (2) is very problematic because experimental luminescence spectra are most often obtained not in the configuration coordinates R, but in the coordinates of photon energies or wavelengths (the left-hand side of expression (1)). To recalculate expression (8) into expression (7), we have to know the quantities R', R_1, and R_2, as well as the coefficients α and β of the configuration parabolas, which change the position and shape of curve *4* in Fig. 1 and depend on the researched material and the specific luminescence center, which is associated with the corresponding individual band included in formula (1).

It should be noted that the indicated quantities do not usually enter the kit of input data. On the contrary, they are determined by analyzing experimental results obtained for examined materials. For example, the quantity R' can be expressed in terms of the radiation, $E_{R'}$, and absorption, E_{ab}, energies, which are usually determined experimentally, using the formula

$$R' = \sqrt{\frac{E_{ab} - E_{R'}}{\alpha + \beta}}. \tag{9}$$

Theoretical calculations of all the above-mentioned constants and coefficients (R', R_1, R_2, α, and β) for each type of luminescence centers and every specific material are very difficult. Therefore, when applying expressions (1) and (2) in practice, it is necessary to use approximate methods for the selection of the approximating function $f(x)$.

It is obvious that the luminescence spectra of individual bands can have a Gaussian distribution (curve *5* in Fig. 1) only if the sections of the parabolas describing the ground and excited states of the luminescence center (curves *1* and *2* in Fig. 1) can be replaced by straight line segments. In this case, the straight line segment corresponding to the excited state will be parallel to the abscissa axis, and the straight line segment replacing the ground-state parabola will be tangent to the parabola at the point with the coordinates $(E_{R'}, R')$. Then, the greatest coincidence between the parabola and the straight line will take place at the point corresponding to the maximum of the individual band in the experimental spectrum. In this case, the maxima of curves *4* and *5* will coincide, as is shown in Fig. 1.

In the coordinates of our model, the equations of the straight lines describing the ground and excited states are

$$\begin{aligned} &E_1(R) = E_1^{\text{line}}(R) = kR - E_0 = \alpha R'^2 \frac{R - R''}{R' - R''}; \\ &E_2(R) = \alpha R'^2 + E_{R'}. \end{aligned} \tag{10}$$

In the examined case, $E_2(R) = \text{const}$. The corresponding quantities k and E_0 are

$$\begin{aligned} &k = \frac{\alpha R'^2}{R' - R''}; \\ &E_0 = \alpha R'^2 \frac{R''^2}{R' - R''}. \end{aligned} \tag{11}$$

As a result and taking Eqs. (10) and (11) into account, the transition energy looks like

$$\begin{aligned} &E_{h\nu}^{\text{line}}(R) = E_2(R) - E_1(R) = \\ &= E_{R'} + \alpha R'^2 \left(1 - \frac{R - R''}{R' - R''}\right). \end{aligned} \tag{12}$$

From formula (12), it is obvious that the transition energy depends linearly on the configuration coordinate R. Taking into account Eq. (12), the approximating function $f(x)$, being expressed in terms of the configuration coordinate R, has a Gaussian shape (curve *5* in Fig. 1) and takes the form

$$\begin{aligned} &f^{\text{line}}(x) = N^{\text{line}}(E_{h\nu}^{\text{line}}) = \\ &= A_E \exp \frac{-\left[E_{h\nu}^{\text{line}}(R) - E_{R'}\right]^2}{2\omega_R^{\text{line }2}}. \end{aligned} \tag{13}$$

in the selected coordinates of the individual bands. In formula (13),

$$\omega_R^{\text{line}} = E_{h\nu}^{\text{line}}(R_1) - E_{h\nu}^{\text{line}}(R_2) = k(R_2 - R_1)$$

is the half-width and

$$A_E = \frac{p}{\sqrt{2}\pi\omega_R^{\text{line}}} = \frac{p}{\sqrt{2}\pi k(R_2 - R_1)}$$

the amplitude of the individual-band maximum (here p is the proportionality coefficient between the probability density function of the normal distribution (curve *3* in Fig. 1) and the quantity $N^{\text{line}}(E_{h\nu})$). Then,

$$\begin{aligned} &N^{\text{line}}(R) = \frac{p}{\sqrt{2}\pi \frac{\alpha R'^2}{R' - R''}(R_2 - R_1)} \times \\ &\times \exp \frac{-\left[\alpha R'^2 \left(1 - \frac{R - R''}{R' - R''}\right)\right]^2}{2\left[\frac{\alpha R'^2}{R' - R''}(R_2 - R_1)\right]^2} = \\ &= \frac{p}{\sqrt{2}\pi \frac{\alpha R'^2}{R' - R''}(R_2 - R_1)} \exp \frac{[R' - R]^2}{2[R_2 - R_1]^2}. \end{aligned} \tag{14}$$

As one can see from formula (14), $N^{\text{line}}(R)$ has the form of a symmetric Gaussian function of R'. The area of the figures ABL and $A_1B_1L_1$ in Fig. 1 can be considered as the error of the approximating function selection for an individual band. The minimum of these errors for all individual bands in the experimental spectrum will accordingly provide the minimum value for the total deviation error of the sum of approximating functions from the values of the experimental luminescence spectrum.

In model (1), the selection of the half-widths ω_i and amplitudes A_i of the approximated individual bands, if the positions of their maxima are known, is also carried out by minimizing the value of the total error $\Delta\varphi(x)$ using formula (2). The optimal values of A_i and ω_i are those that make it possible to obtain curves $f_i(x)$ in (1) that best match curve *5* in Fig. 1. Additionally, instead of calculating the transition energies

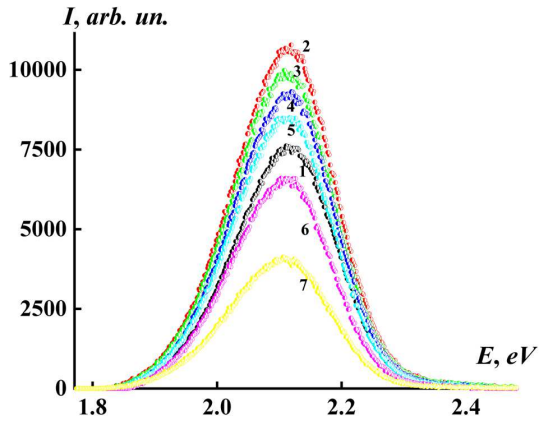

Fig. 2. Experimental PL spectra of Mn^{2+} ions in ZnS single crystals with the PD degree $\varepsilon = 0\%$ (*1*), 1.4% (*2*), 4.22% (*3*), 8.8% (*4*), 17.96% (*5*), and 25% (*6*). $C_{Mn} = 10^{-2}$ gMnS/gZnS, $E_{ex.} = 2.55$ eV ($\lambda_{ex.} = 408$ nm)

and half-widths in terms of the configuration coordinate R, as is shown in expression (14), by assuming that the transition energy depends linearly on the configuration coordinate and using Eq. (2), the values of the parameters ω_i (half-widths) and A_i (amplitudes) of the approximated individual bands are optimized using the known positions of their maxima. The application of this approach gives an error associated with neglecting the curvature of the ground- and excited-state levels. However, if we assume that the majority of charge carriers in the excited state are near the minimum of curve *2* in a small interval of R-values (Fig. 1), then this error associated with the excited-state curvature will also be small.

3. Experimental Part

To experimentally verify the possibility of resolving experimental spectra into individual components using a normal distribution, ZnS single crystals doped with Mn^{2+} ions were used. It is known that the experimental PL spectra of these single crystals are the total emission of several individual luminescence bands overlapping one another. Each of those bands is associated with the emission by Mn^{2+} ions with a certain local symmetry. The type of local symmetry associated with each band, the number of bands, and the positions of their maxima were described in works [14–16, 20, 21]. According to those data, the individual PL band with a maximum at $\lambda_{max} = 557$ nm ($E_{h\nu\ max} = 2.23$ eV) is associated with the emission by Mn^{2+} ions located in stacking faults with the local C_3v symmetry (the AS- and PN-type sites) and in a field with the local cubic Td symmetry (the AN-type sites) [14, 21]. The individual band at $\lambda_{max} = 557$ nm ($E_{h\nu\ max} = 2.15$ eV) is associated with the emission by Mn^{2+} ions located near dislocations and point defects [14–16]. The emission of the band at $\lambda_{max} = 600$ nm ($E_{h\nu\ max} = 2.07$ eV) is related to the emission by manganese centers located in a local cubic environment at octahedral interstitials [14, 15, 20]. According to work [20], the individual band at $\lambda_{max} = 635$ nm ($E_{h\nu\ max} = 1.96$ eV) is associated with the emission from the intercalated α-MnS phase in ZnS.

The influence of plastic deformation (PD) on the photoluminescence (PL) spectra of individual bands of Mn^{2+} ions, which have a monomolecular (intracenter) luminescence character, was studied. The experiments were aimed at obtaining information about variations in the luminescence properties of this material by constructing quantitative models that provide an understanding of changes in the relative number of luminescent Mn^{2+} ions and their dependence on the plastic deformation degree ε. The normal distribution over the photon-energy coordinates was used as an approximation function in one case, and the normal distribution over the wavelength coordinates along the abscissa axis in the other.

A semiconductor laser with an exciting light energy of $E_{ex.} = 2.55$ eV ($\lambda_{ex.} = 408$ nm) was used as an excitation source. The radiation power at the specimen location was approximately 10 mW. The radiation was registered using a measuring complex of the KSVU-5-type, which included a monochromator with a set of variable diffraction gratings and a FEP-136 photomultiplier. The maximum resolution of the radiation registration was approximately 0.1 nm. The PL intensity was measured in the photon counting mode and was presented as a set of experimental values characterizing the intensity dependence on the PL radiation wavelength, measured with equivalent increments of 0.5 nm along the wavelength axis. The intensity values (Fig. 2) and the areas under the curves of individual PL bands (the integral brightness S_i) along the ordinate axis are presented in conventional units that are proportional to the number of photons, and the wavelengths are converted into photon energies (the abscissa axis).

The specimens were obtained by cleavage from large blocks of ZnS : Mn single crystals grown from the melt under an argon pressure of 150 atm, and they had a microtwin structure. The activator concentration $C_{\rm Mn} = 10^{-2}$ gMnS/gZnS (the concentration of initial impurities in the charge) was chosen taking into account the implementation of both direct optical and resonance excitation mechanisms of Mn^{2+} ion luminescence centers in ZnS single crystals. In our studies, the selected excitation energy $E_{\rm ex.} = 2.55$ eV ($\lambda_{\rm ex.} = 408$ nm) corresponded to one of the PL excitation bands of Mn^{2+} ions in ZnS single crystals, which allowed the direct optical mechanism of PL excitation of Mn^{2+} ions to be implemented in the studied single crystals. On the other hand, at this $C_{\rm Mn}$-value, the distances between MCs are sufficient for their resonance interaction with one another, and the implementation of the resonance excitation mechanism is also quite possible. In addition, the effect of concentration PL quenching is practically absent [22].

The initial dimensions of the polished specimens subjected to deformation were $1.8 \times 1.8 \times 3.6$ mm^3. The deforming stress was applied at an angle of 45° with respect to the $(111)_C$ slip plane. The PD procedure was carried out at the temperature $T = 423$ K and at a rate of about 5×10^{-8} m/s. The obtained experimental spectra are shown in Fig. 2.

Each experimental spectrum was resolved into individual PL bands. During this procedure, the deviations of the plot for the sum of the functions approximating the individual bands from the total experimental PL spectrum did not exceed 1.5÷1.7% of the maximum PL intensity (Fig. 3).

As a result of the resolution, the values of the integral brightness S_i were obtained by calculating the area under the plot of each individual PL band (Fig. 4), as well as the relative numbers N_i of Mn^{2+} luminescence centers with different local environments in the ZnS crystal lattice (Fig. 5) at various ε-values. In Fig. 5, the N_i-values are expressed in the units corresponding to the relative number of the relevant luminescence centers in undeformed single crystals.

An analysis of the obtained results allowed us to trace the behavior of individual bands during the PD process in a rather informative manner and to obtain information about the relative quantitative changes over time of the parameters of luminescence centers of different types. Taking into account different local

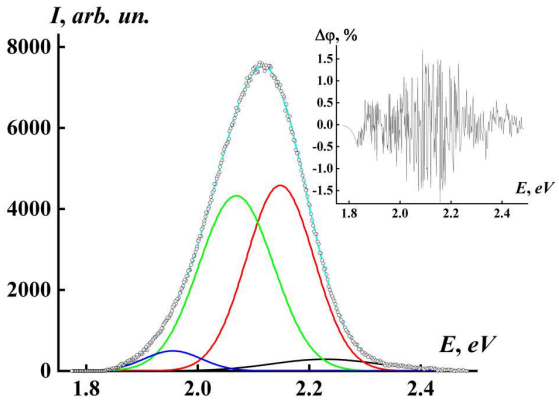

Fig. 3. Resolution of the PL spectrum of a ZnS:Mn single crystal into separate bands with $E_{h\nu\ \rm max} = 2.23$, 2.15, 2.07, and 1.96 eV ($\lambda_{\rm max} = 557$, 578, 600, and 635 nm, respectively). $C_{\rm Mn} = 10^{-2}$ gMnS/gZnS, $E_{\rm ex.} = 2.55$ eV ($\lambda_{\rm ex.} = 408$ nm), $\varepsilon = 0$. Points represent an experimental total PL spectrum, and curves are calculated intensities of individual PL bands and their sum. The deviations ΔA of the resolution envelope from the experimental spectrum are shown in the inset

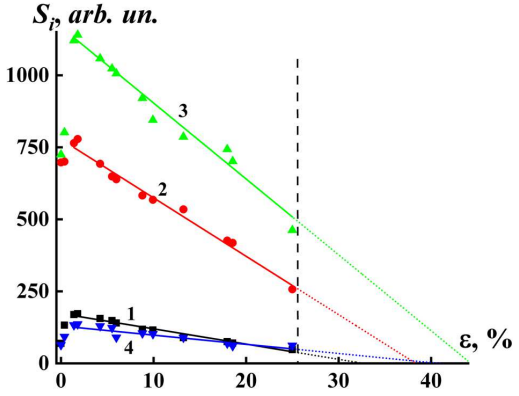

Fig. 4. Dependences of the integral brightness S_i of individual MC bands in ZnS : Mn single crystals on the PD degree ε obtained by resolving experimental PL spectra. $E_{\rm ex.} = 2.55$ eV ($\lambda_{\rm ex.} = 408$ nm), $C_{\rm Mn} = 10^{-2}$ gMnS/gZnS, $\lambda_{\rm max} = 557$ (*1*), 578 (*2*), 600 (*3*), and 635 nm (*4*). The vertical dashed line marks the approximate PD value ε corresponding to specimen destruction. Linear decreasing sections of S_i are approximations at PD values before (solid lines) and after (dashed lines) specimen destruction

environments of the Mn^{2+} luminescence centers in the ZnS crystal lattice, this analysis made it possible to trace the deformation changes in the researched single crystals to a certain extent. In addition, the possibility of a correlation between the obtained results and the results of previous studies dealing with deformation changes in ZnS single crystals with an admix-

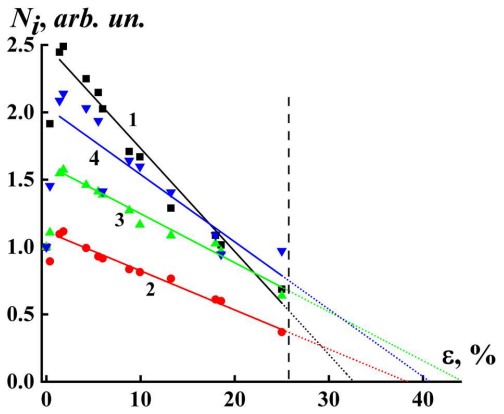

Fig. 5. Dependences of the relative quantity N_i of Mn^{2+} luminescence centers in ZnS single crystals, which are related to the emission of certain individual bands with $\lambda_{max} = 557$ (*1*), 578 (*2*), 600 (*3*), and 635 nm *(4)* obtained by resolving experimental PL spectra, on the PD degree ε. $E_{ex.} = 2.55$ eV ($\lambda_{ex.} = 408$ nm), $C_{Mn} = 10^{-2}$ gMnS/gZnS. The vertical dashed line marks the approximate PD value corresponding to specimen destruction. Linear decreasing sections are approximations at PD values before (solid lines) and after (dashed lines) specimen destruction

ture of Mn^{2+} ions and using other, non-luminescent methods [23–27] was analyzed. In particular, at the initial PD stages, at $\varepsilon \approx 3 \div 5\%$, the values of S_i increased for both the integrated experimental PL spectrum and the spectra of all individual bands. However, the S_i-values for individual bands changed differently. The S_i-value for the integrated experimental spectrum increased by approximately 40%, but this quantity increased by 25–50% for individual bands with $E_{h\nu\ max} = 2.15$ and 2.07 eV, and by 1.2–1.6 times for individual bands with $E_{h\nu\ max} = 2.23$ and 1.96 eV. If the PD grew further, the S_i-value decreased almost linearly until the specimen destruction, similarly to the behavior of the electron paramagnetic resonance (EPR) curves associated with Mn^{2+} ions in the hexagonal environment of the ZnS crystal lattice [26]. The decrease rate $\Delta S_i/\Delta\varepsilon$ depended on the type of individual PL band. The extrapolation of the linear decrease of the S_i-value to deformation values exceeding the specimen destruction threshold made it possible to predict the behavior of individual PL bands in this deformation region (Figs. 4 and 5).

By comparing the obtained results with the EPR data from works [23–27], we can notice a certain correlation between them. According to the results of the cited works, during the PD process of ZnS single crystals with an admixture of Mn^{2+} ions, the dislocation motion brought about changes in the crystal structure and a defectiveness reduction in the deformed single crystals [23–25]. The crystal structure was restructured from a microtwin one and polytypes into the unidirectional cubic structure of sphalerite. The PD process was accompanied by an almost vanishing number of stacking faults at the PD degree $\varepsilon \approx 18.2\%$ [26,27]. At the same time, at small PD values, the EPR lines behaved anomalously, which was attributed to the emergence of some disordered structure owing to the initial displacements of dislocations from their positions [26].

All those events can be observed in the results of our studies. For instance, the unusual behavior of the shape and width of the EPR lines at the initial PD stages, which was associated by the cited authors with the emergence of some disordered structure, also takes place in our PL spectra of individual bands in the form of the intensity (Fig. 2) and integral brightness (Fig. 4) jumps in the same region of small PD values. The linear reduction in the intensity of EPR lines, which are associated with the hexagonal environment of Mn^{2+} ions in the ZnS crystal lattice, and the number of stacking faults [26] are observed as a similar decrease of the S_i- and N_i-values for all individual bands.

The behavior of individual bands can also be analyzed. For example, the individual band at $\lambda_{max} = 557$ nm ($E_{h\nu\ max} = 2.23$ eV) is associated with the emission by Mn^{2+} ions located in stacking faults. The number of such emission centers during the PD process decreases due to a reduction in the overall specimen defectiveness and the number of sensitization centers near manganese centers, which reduces the probability of radiative transitions in the Mn^{2+} ions themselves.

The individual band at $\lambda_{max} = 578$ nm ($E_{h\nu\ max} = 2.15$ eV) is associated with the emission by Mn^{2+} ions located near dislocations and point defects. During the PD process, as a result of the motion of partial dislocations, they exit from the bulk to the surface of the deformed specimen. As a result, the number of emitting manganese centers contributing to the radiation of this individual band decreases.

Non-zero values of the parameters S_i and N_i for all individual bands at $\varepsilon \approx 18.2\%$ can be explained by a discrepancy between the results of the EPR and pho-

toluminescence studies. According to the EPR data, Mn^{2+} ions are distributed in equilibrium over the ZnS crystal lattice [17]. About 90% of them are located in the tetrahedral environment, and the other 10% are located in stacking faults with the hexagonal and trigonal environments in the ZnS crystal lattice. Just these manganese ions are associated with the emission of an individual band at $\lambda_{\max} = 557$ nm ($E_{h\nu\ \max} = 2.23$ eV) [7, 8, 13]. This band has the smallest S_i- and N_i-values and decreases most substantially in comparison with all other bands during the PD process. Nevertheless, less than 1% of the total number of Mn^{2+} ions in ZnS is associated with the emission to the most intensive individual bands [28]. Just these individual bands have the largest S_i- and N_i-values and make the main contribution to the integral PL spectrum.

All Mn^{2+} ions, both emitting and non-emitting, contribute to the EPR signal. Therefore, the statement that the PD process is accompanied by an almost total reduction in the number of stacking faults at the PD degree $\varepsilon \approx 18.2\%$ in the case of the EPR signal [26, 27] is not valid (this is not zero at all) in the case of the PL signal. Furthermore, not all partial dislocations moving over the crystal subjected to PD reach the crystal surface. Some of them remain in the bulk due to various reasons (for example, due to braking and stopping [10]), which are responsible for the non-zero values of the quantities S_i and N_i at $\varepsilon \approx 18.2\%$.

4. Conclusions

To summarize, as a result of the performed research using the configurational coordinate model, it has been shown that it is appropriate to apply the normal distribution for the description of the shape of individual bands when resolving luminescence spectra into individual components. The normal distribution in the coordinates of photon energies along the abscissa axis is close to theoretical concepts about the luminescence band shape and allows such a resolution to be carried out with a certain accuracy. However, taking into account that there are always some phonon-induced or other effects, which are difficult to take into account in the model, but which also affect the shape of the individual band, the final answer concerning the curve shape for the description of individual bands is the subject of further research. The results obtained for the behavior of individual photoluminescence bands of ZnS single crystals with an admixture of Mn^{2+} ions made it possible to trace the behavior of individual bands and, to some extent, changes in the relative quantitative characteristics of emitting manganese centers with various local environments during the PD process. The results correlate with the results of EPR studies obtained during the PD process; they supplement information on the methods for resolving experimental luminescence spectra into individual components and do not contradict generally accepted concepts about the photoluminescence mechanisms in single-crystalline materials of the A_2B_6-type.

1. V.I. Budyanskii, D.S. Lepsveridze, E.A. Salkov, G.A. Shepelskii. Differential luminescence spectrum. *Fiz. Tverd. Tela* **15**, 1620 (1973) (in Russian).
2. M.V. Fock. Resolution of complicated spectra into individual bands using the Alentsev method. *Trudy FIAN SSSR* **59**, 3 (1972) (in Russian).
3. A.V. Kovalenko, E.G. Plakhtiy, S.M. Vovk. Application of derivative spectroscopy method to photoluminescence in ZnS:Mn nanocrystals. *Ukr. J. Phys. Optics* **19**, 133 (2018).
4. A.V. Kovalenko, S.M. Vovk, E.G. Plakhtiy. Method for decomposing the sum of Gaussian functions constituting the experimental photoluminescence spectrum. *J. Appl. Spectrosc.* **88**, 297 (2021).
5. B.V. Shulgin, A.N. Tcherepanov, V.Yu. Ivanov, T.S. Koroleva, M.M. Kidibaev, Ch. Pedrini, Ch. Dujardin. Luminescence spectroscopy of NaF: U bulk and fiber crystals. *J. Luminesc.* **125,** 259 (2007).
6. A.S. Babkin, E.A. Seregina, A.A. Seregin, G.V. Tikhonov. Spectral and luminescent properties of Yb^{3+} in aprotic inorganic liquids $POCl_3$–$ZrCl_4$. *Opt. Spektrosk.* **125**, 507 (2018) (in Russian).
7. S.S. Novosad, I.S. Novosad, B.M. Kalivoshka. Luminescent and photochemical processes in $CdBr_2 : AgCl$ crystals. *Fiz. Tverd. Tela* **53**, 1548 (2011) (in Russian).
8. T.A. Prokofiev, A.V. Ivanchenko, V.V. Gnatushenko. Luminescence analysis of crystal lattice changes in ZnS single crystals doped with Mn^{2+} ions during plastic deformation. **86**, 195 (2019) (in Russian).
9. T.A. Prokofiev, A.V. Ivanchenko. Temperature dependences of photoluminescence of Mn^{2+} ions with various local environments in ZnS single crystals. *Zh. Prikl. Spektrosk.* **87**, 561 (2020) (in Russian).
10. T.A. Prokof'ev, O.V. Ivanchenko. The influence of dislocation inhibition duting plastic deformation on the photoluminescence of Mn^{2+} ions in ZnS single crystals. *Ukr. Fiz. Zh.* **67**, 202 (2022) (in Ukrainian).
11. E.S. Wentzel. *Probability Theory: First Steps* (Mir, 1982).
12. J.H. Williams. *Quantifying Measurement: The Tyranny Of Numbers* (Morgan and Claypool Publishers, 2016).
13. Y. Bard. *Nonlinear Parameter Estimation* (Academic Press, 1974).

14. H.E. Gumlich. Electro- and photoluminescence properties of Mn^{2+} in ZnS and ZnCdS. *J. Luminesc.* **23**, 73 (1981).
15. G.E. Arkhangelsky, N.N. Grigoriev, M.V. Fok, N.A. Yakunina. The influence of plastic deformation for luminescence and electron paramagnetic resonance of ZnS-Eu crystals. *Trudy FIAN SSSR* **164**, 43 (1985) (in Russian).
16. M.F. Bulanyi, B.A. Polezhaev, T.A. Prokofiev. About the nature of manganese luminescence centers in zinc sulfide single crystals. *Fiz. Tekh. Poluprovodn.* **32**, 673 (1998) (in Russian).
17. G.E. Arkhangelskii, E.E. Bukke, T.I. Voznesenskaya, N.N. Grigoriev, M.V. Fok. Visualization of structural distortions in ZnS-type crystals by decorating with anthraquinone. In: *Methods of Image Visualization* (Nauka, 1981), p. 66 (in Russian).
18. A.Ya. Yakunin, I.V. Shtambur, A.S. Kushnir, A.S. Omelchenko. EPR spectra of Mn^{2+} in normal and defect sites of ZnS crystal lattice. *Izvestiya Vuzov Fiz.* **10**, 44 (1973) (in Russian).
19. W. Busse, H.E. Gumlich, R.O. Tornqvist, V.P. Tanninan. Zero-phonon lines in electroluminescence and photoluminescence of ZnS: Mn thin films grown by atomic layer epitaxy. *Phys. Status Solidi A* **76**, 553 (1983).
20. N.D. Borisenko, M.F. Bulanyi, F.F. Kodzhespirov, B.A. Polezhaev. Properties of luminescence centers in zinc sulfide single crystals with manganese impurity. *Zh. Prikl. Spektrosk.* **55**, 452 (1991) (in Russian).
21. M.F. Bulanyi, A.V. Kovalenko, B.A. Polezhaev. Spectra of manganese luminescence centers in zinc sulfide. *Zh. Prikl. Spektrosk.* **69**, 747 (2002) (in Russian).
22. T.A. Prokofiev, B.A. Polezhaev, A.V. Kovalenko. Mechanisms of photoluminescence excitation of Mn^{2+} Ions in ZnS crystals. *Zh. Prikl. Spektrosk.* **72**, 788 (2005) (in Russian).
23. *Electronic Properties of Dislocations in Semiconductors.* Edited by Yu.A. Osip'yan (Editorial URSS, 2000) (in Russian).
24. B.A. Abdikamalov, S.I. Bredikhin, M.P. Kulakov, V.Sh. Shekhtman, S.Z. Shmurak. Phase transition at plastic deformation of zinc sulfide crystals. *Fiz. Tverd. Tela* **18**, 2463 (1976) (in Russian).
25. S.I. Bredikhin, S.Z. Shmurak. Luminescence of plastically deformed ZnS crystals. *Zh. Èksp. Teor. Fiz.* **73**, 1460 (1977) (in Russian).
26. S.I. Bredikhin, S.A. Omelchenko, S.Z. Shmurak, N.A. Yakunina. EPR of Mn^{2+} in plastically deformed ZnS single crystals. *Fiz. Tverd. Tela* **23**, 903 (1981) (in Russian).
27. S.A. Omelchenko, S.I. Bredikhin, P.A. Berlov, M.F. Bulany, S.Z. Shmurak, A.Ya. Yakunin. Kinetics of deformation-induced structural reorientation in zinc sulfide and selenide crystals. *Fiz. Tverd. Tela* **24**, 2803 (1982) (in Russian).
28. N.D. Borisenko, M.F. Bulanyi, B.A. Polezhaev. Plastic deformation effect on photoluminescence of ZnS : Mn crystals. *Zh. Prikl. Spektrosk.* **50**, 847 (1989) (in Russian).

Received 10.03.25.

Translated from Ukrainian by O.I. Voitenko

Т.А. Прокоф'єв, О.В. Іванченко

ПРО ФОРМУ КРИВОЇ ТА ВИБІР КООРДИНАТ ПРИ РОЗКЛАДАННІ СПЕКТРІВ ЛЮМІНЕСЦЕНЦІЇ НА ОКРЕМІ СКЛАДОВІ

За допомогою моделі конфігураційних координат проаналізовано можливість використання для апроксимації спектрів люмінесценції виокремлених смуг нормального розподілу в координатах енергій фотонів. Практичне застосування цього підходу для монокристалів ZnS з домішкою іонів Mn^{2+} дозволило отримати спектри фотолюмінесценції окремих смуг для різних значень величини пластичної деформації. З урахуванням залежності площі під кривою окремої смуги від кількості центрів світіння це вдалося певним чином простежити за зміною відносних кількісних характеристик випромінюючих марганцевих центрів з різним локальним оточенням у процесі пластичної деформації. Отримані результати корелюють з результатами досліджень електронного парамагнітного резонансу, доповнюють інформацію про методи розкладання експериментальних спектрів люмінесценції на окремі складові та не суперечать загальноприйнятим уявленням про механізми фотолюмінесценції монокристалічних матеріалів типу A_2B_6.

Ключові слова: спектри люмінесценції, смуги люмінесценції, модель конфігураційних координат, розкладання спектрів люмінесценції на окремі складові, помилка розкладання експериментальних спектрів люмінесценції, пластична деформація.